Human CalDAG-GEFI gene (*RASGRP2*) mutation affects platelet function and causes severe bleeding

Matthias Canault,[1,2,3] Dorsaf Ghalloussi,[1,2,3] Charlotte Grosdidier,[1,2,3] Marie Guinier,[4] Claire Perret,[5,6,7] Nadjim Chelghoum,[4] Marine Germain,[5,6,7] Hana Raslova,[8] Franck Peiretti,[1,2,3] Pierre E. Morange,[1,2,3] Noemie Saut,[1,2,3] Xavier Pillois,[9,10] Alan T. Nurden,[10] François Cambien,[5,6,7] Anne Pierres,[3,11,12] Timo K. van den Berg,[13] Taco W. Kuijpers,[13] Marie-Christine Alessi,[1,2,3] and David-Alexandre Tregouet[5,6,7]

[1]Institut National de la Santé et de la Recherche Médicale (Inserm), UMR_S 1062, 13005 Marseille, France
[2]Inra, UMR_INRA 1260, 13005 Marseille, France
[3]Aix Marseille Université, 13005 Marseille, France
[4]Post-Genomic Platform of Pitié-Salpêtrière (P3S), Pierre and Marie Curie University, F-75013 Paris, France
[5]Sorbonne Universités, UPMC Univ Paris 06, UMR_S 1166, F-75013 Paris, France
[6]Inserm, UMR_S 1166, Team Genomics and Pathophysiology of Cardiovascular Diseases, F-75013 Paris, France
[7]ICAN Institute for Cardiometabolism and Nutrition, F-75013 Paris, France
[8]Hématopoïèse Normale et Pathologique, Inserm Médicale U1009, 94805 Villejuif, France
[9]LIRYC, Plateforme Technologique et d'Innovation Biomédicale, Hôpital Xavier Arnozan, Pessac, France
[10]Inserm, UMR_1034, 33600 Pessac, France
[11]Inserm, UMR_1067, 13288 Marseille, France
[12]CNRS UMR_7333, 13288 Marseille, France
[13]Department of Blood Cell Research, Sanquin Research and Landsteiner Laboratory, Academic Medical Center, University of Amsterdam, 1105 AZ Amsterdam, Netherlands

The nature of an inherited platelet disorder was investigated in three siblings affected by severe bleeding. Using whole-exome sequencing, we identified the culprit mutation (cG742T) in the *RAS guanyl-releasing protein-2* (*RASGRP2*) gene coding for calcium- and DAG-regulated guanine exchange factor-1 (CalDAG-GEFI). Platelets from individuals carrying the mutation present a reduced ability to activate Rap1 and to perform proper αIIbβ3 integrin inside-out signaling. Expression of CalDAG-GEFI mutant in HEK293T cells abolished Rap1 activation upon stimulation. Nevertheless, the PKC- and ADP-dependent pathways allow residual platelet activation in the absence of functional CalDAG-GEFI. The mutation impairs the platelet's ability to form thrombi under flow and spread normally as a consequence of reduced Rac1 GTP-binding. Functional deficiencies were confined to platelets and megakaryocytes with no leukocyte alteration. This contrasts with the phenotype seen in type III leukocyte adhesion deficiency caused by the absence of kindlin-3. Heterozygous did not suffer from bleeding and have normal platelet aggregation; however, their platelets mimicked homozygous ones by failing to undergo normal adhesion under flow and spreading. Rescue experiments on cultured patient megakaryocytes corrected the functional deficiency after transfection with wild-type *RASGRP2*. Remarkably, the presence of a single normal allele is sufficient to prevent bleeding, making CalDAG-GEFI a novel and potentially safe therapeutic target to prevent thrombosis.

CORRESPONDENCE
Marie-Christine Alessi:
marie-christine.alessi@univ-amu.fr

Abbreviations used: CalDAG-GEFI, calcium- and DAG-regulated GEF-1; *FERMT3*, *fermitin family member 3*; GEF, guanine exchange factor; Ha-ras, Harvey rat sarcoma viral oncogene homolog; PRP, platelet-rich plasma; *RASGRP2*, *RAS guanyl-releasing protein-2*; SRC, structurally conserved domain.

Inherited platelet disorders are rare diseases that give rise to bleeding when platelets fail to fulfill their hemostatic function upon vessel injury. Clinical manifestations include mainly mucocutaneous bleeding, menometrorrhagia and excessive bleeding after surgical intervention or trauma. The study of these diseases allows a better understanding of normal platelet biochemistry

M.-C. Alessi and D.-A. Tregouet contributed equally to this paper.

The Rockefeller University Press $30.00
J. Exp. Med. 2014 Vol. 211 No. 7 1349-1362
www.jem.org/cgi/doi/10.1084/jem.20130477

The Journal of Experimental Medicine

and physiology. These inherited disorders include abnormalities of platelet receptors, granules, or signal transduction (Nurden and Nurden, 2011). Signal transduction dysfunction is thought to be the most common cause of platelet inherited disorders; however, only a few have been successfully genotyped.

Here, we have identified and characterized the first mutation of *RASGRP2* (RAS guanyl-releasing protein-2) in a family suffering severe bleeding. *RASGRP2* codes for a major signaling molecule in platelets, calcium-and-DAG-regulated guanine exchange factor-1 (CalDAG-GEFI). It is a guanine nucleotide exchange factor (GEF) that is critical for Ras-like GTPase activation whose target is mainly Rap1 in platelets (Crittenden et al., 2004; Bergmeier et al., 2007; Cifuni et al., 2008; Stefanini et al., 2009). Rap1 is one of the most predominant small GTPases in platelets and constitutes a key signaling element that governs platelet activation by directly regulating integrin-mediated aggregation and granule secretion (Chrzanowska-Wodnicka et al., 2005; Zhang et al., 2011). Mice lacking CalDAG-GEFI not only have major defects in platelet function, with a reduced ability to form thrombi upon vascular injury, but they also have impaired neutrophil functions (Crittenden et al., 2004; Bergmeier et al., 2007; Carbo et al., 2010). To date, no pathological mutation in *RASGRP2* has been reported in man and knowledge about the phenotype linked to human CalDAG-GEFI deficiency is lacking.

RESULTS

Initial characterization of the patients

We report here the cases of three siblings (two males and one female) from consanguineous parents (first cousins) that were born between 1957 and 1962 after asymptomatic pregnancies. All suffered from mucocutaneous bleeding starting at 18 mo; these episodes consisted mainly of prolonged and severe epistaxis, hematomas, and bleeding after tooth extraction. The clinical presentation of the female was more severe due to massive menorrhagia and chronic anemia that were controlled by oestroprogestogenic therapy. Two of them required recurrent blood transfusions until adolescence. One of the patients successfully received transfusion of platelet concentrates before soft tissue surgery to prevent bleeding. Bleeding times tested on several occasions were always prolonged (>20 min). Interview and clinical examination of the parents, two other siblings, and the two children of one of the patient did not reveal any bleeding tendency. The bleeding times measured in the two unaffected siblings were normal (5–6 min). Initial platelet screening in patients demonstrated a reduced maximal aggregation in response to all tested doses of ADP or epinephrine and to low doses of thrombin receptor–activating peptide-14 (TRAP-14) and collagen, whereas aggregation with ristocetin or phorbol myristate acetate (PMA) was normal (Fig. 1 a). When induced by high-dose arachidonic acid, TRAP-14, or collagen, maximal aggregation was comparable to controls (Fig. 1 a). Notably, aggregation velocities were lower for the patient's platelets as compared with healthy control platelets with all tested ADP doses and even at high doses of TRAP-14 and collagen (Fig. 1 b). Expression of all studied membrane receptors, including αIIbβ3 and GPIbα, were normal (Fig. 1 c). Binding of the αIIbβ3 activation-specific antibody, PAC-1, was identical for patients and controls at high (Fig. 1 c) and low (not depicted) doses of TRAP-14 and ADP. Platelet granule content and release were assayed. Platelet serotonin and PAI-1 contents, mepacrine uptake/release, and granulophysin (CD63) surface expression were normal upon high-dose agonist stimulation (ADP 10 µM and TRAP-14 50 µM; unpublished data). P-selectin surface expression tended to be lower in patients at high- (Fig. 1 c) and low-dose (not depicted) agonists. These results indicate normal contents of dense, α-, and lysosomal granules, albeit with a slightly reduced α-granule secretion. Clot retraction, induced by 1 U/ml thrombin was not affected (unpublished data). Thrombin generation in platelet-rich plasma (PRP) depends on platelet activation and αIIbβ3 activation as much as it does on the plasma clotting factors (Reverter et al., 1996; Hemker et al., 2006; van der Meijden et al., 2012). In the patients, thrombin generation in PRP was moderately affected with a delayed time to peak but a normal total amount of generated thrombin (Fig. 1 d) and no difference in phosphatidylserine exposure induced by TRAP-6/collagen stimulation (unpublished data).

Overall, these data indicate a selective change in platelet-signaling pathways mainly seen at low dose of agonists.

A mutation in the RASGRP2 gene is responsible for the bleeding phenotype

To identify the molecular defect hypothesized to follow a recessive inheritance model, we sequenced the exomes of two affected siblings and three nonaffected relatives, including both parents. Focusing on single nucleotide or ins/del variants affecting coding regions, 114 candidate variants were found to follow the recessive hypothesis. From these, we selected candidates that were absent or at low frequency (<1%) in public databases including the 1,000 Genomes projects and the Exome Variant Server (December 2011 releases). This resulted in a list of four candidates (Table 1); among these one clearly stood out, a nonsynonymous c.G742T mutation within the exon 8 of the *RASGRP2* gene, leading to a glycine-to-tryptophan substitution at position 248 (p.G248W; Fig. 2 a). CalDAG-GEFI is composed of four domains including the CDC25 catalytic domain (Kawasaki et al., 1998) containing five structurally conserved regions (SCRs) critical for its interaction with the GTPases. The mutation we describe here is located in the sequence encoding SCR2 of CDC25 of CalDAG-GEFI and was predicted by the PolyPhen-2 software to have functional consequences on the encoded protein. *RASGRP2* genotypes were confirmed by capillary sequencing to segregate with the disease in the whole family (Fig. 2, b and c). Sequence alignment analysis did not reveal any cryptic site introduced by the c.G742T mutation that could have resulted in a truncated splicing form. Accordingly, quantitative real time-PCR and Western blot analysis showed normal CalDAG-GEFI mRNA and protein expressions in homozygous carriers of the c.G742T mutation (Fig. 2, d and e).

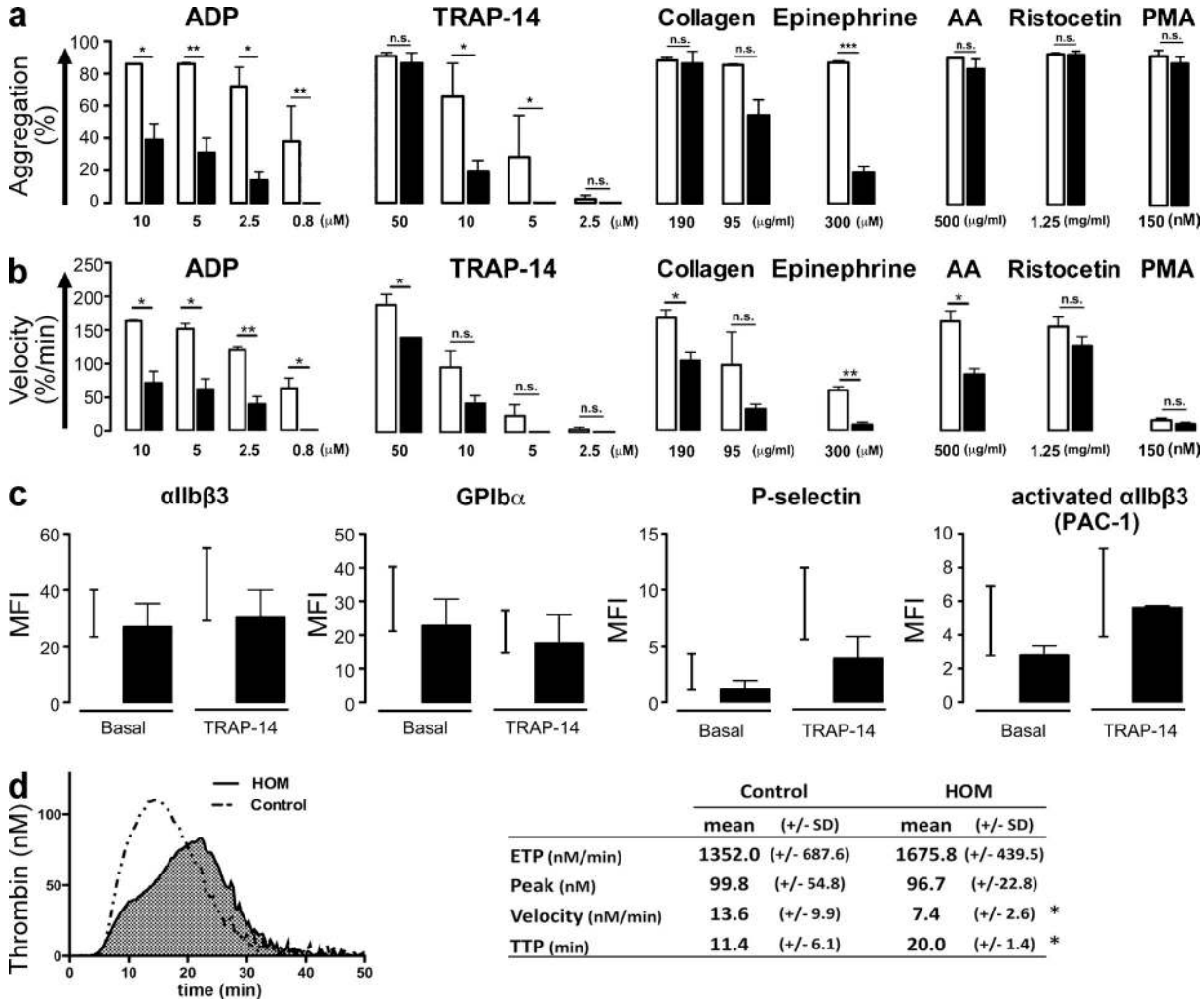

	Control mean	Control (+/- SD)	HOM mean	HOM (+/- SD)	
ETP (nM/min)	1352.0	(+/- 687.6)	1675.8	(+/- 439.5)	
Peak (nM)	99.8	(+/- 54.8)	96.7	(+/-22.8)	
Velocity (nM/min)	13.6	(+/- 9.9)	7.4	(+/- 2.6)	*
TTP (min)	11.4	(+/- 6.1)	20.0	(+/- 1.4)	*

Figure 1. Characterization of the patients' platelet function. (a) Platelet maximal aggregation (%) and (b) velocity (%/min) from 2 patients (filled bars) and 3 healthy volunteers (open bars) induced by ADP, TRAP-14, collagen, epinephrine, arachidonic acid, ristocetin, and PMA tested on 5 different occasions (Student's *t* test; *, P < 0.05; **, P < 0.01; ***, P < 0.001). (c) Levels of αIIbβ3 integrin, GPIbα, P-selectin, and PAC-1 binding (activated αIIbβ3) on resting and TRAP-14 (50 µM)-stimulated platelets from 2 patients measured by flow cytometry and expressed as mean fluorescence intensity (MFI). Black lines represent the range between minimum and maximum MFI obtained from healthy volunteers ($n = 8$). (d) Endogenous thrombin generation in PRP (left) and representative thrombograms (right). Thrombogram parameters: area-under-the-curve or ETP (total thrombin activity during coagulation); peak height (maximal rate of thrombin formation); reaction velocity and time to thrombin peak ($n = 5$ for controls; $n = 2$ for HOM; Student's *t* test, *, P < 0.05).

Initially, mutations in *RASGRP2* were reported as the cause for type III leukocyte adhesion deficiency (LAD-III) causing bleeding and immune deficiency (Alon et al., 2003). Further investigations revealed later that mutations in *fermitin family member 3* (*FERMT3*) encoding kindlin-3 were in fact responsible for LAD-III (Kuijpers et al., 2009). In our patients, we found normal *FERMT3* sequence, normal *ITGA2B* and *ITGB3* sequences encoding αIIbβ3 (unpublished data) and normal kindlin-3 protein expression (unpublished data).

The effect of the p.G248W transition on CalDAG-GEFI structure and function was analyzed by protein sequence modeling. Because the CalDAG-GEFI crystal structure has yet to be reported, the analysis was performed on a closely related structure: Sos-2 (Boriack-Sjodin et al., 1998). Comparison of the protein structure of Sos-2 with that of its counterpart Ha-ras (Fig. 3 a.1) revealed the tight interaction of the CDC25 domain of Sos-2, forming a cavity receiving an α-helix of Ha-ras (Fig. 3 a.2). The observed H-bonds concern amino acids relatively conserved through species and across multiple types of Ras proteins and GEFs (Fig. 3 b). The mutation caused the substitution of a small neutral amino acid by a large polar one (compare Fig. 3 a.2.1 and a.2.2), leading to a protrusion within the cavity of the GEF (compare Fig. 3 a.3 and a.4). This is predicted to result in a less effective GDP-GTP exchange and a shift of Ha-Ras to an inactivated, GDP-bound state.

The p.G248W transition impairs CalDAG-GEFI's ability to activate Rap1

Next, we tested the ability of the mutated CalDAG-GEFI to activate Rap1. Platelets from patients with the p.G248W

Table 1. Identified candidate variants following the recessive inheritance model

Chr	Position	Reference allele	Mutated allele	Gene	Amino acid change	Affected		Unaffected		
						Ind. 05	Ind. 06	Ind. 02 (Father)	Ind. 01 (Mother)	Ind. 04
5	139931629	C	G	SRA1	V110L (rs117757312)	34	21	30	39	NA
11	64506903	C	A	RASGRP2	G248W	36	24	18	41	15
11	66458798	C	T	SPTBN2	R1841Q	21	13	9	21	8
11	67209291	C	G	CORO1B	E123Q	14	14	7	15	6

Reads depth of the identified variants that passed the whole-exome filtering strategy consisting of selecting candidate variants that were nonsynonymous variants, frameshifts/insertions/deletions affecting coding regions, that were absent or reported at a low frequency (<1‰) in public databases (including the 1000 Genomes project and the Exome Variant Server), and that were found in the homozygous state in the two affected siblings (with a minimum depth of 10X) but which were heterozygous in the two unaffected parents. NA indicates that the individual is not carrying the identified variant.

CalDAG-GEFI mutation showed a strongly reduced Rap1 activation. In healthy subjects, a dose-dependent Rap1 activation was observed upon ADP stimulation at the tested time points (1 and 5 min). Only the high dose of TRAP-6 induced Rap1 activation in control platelets. For the homozygous patients, no Rap1 activation was seen with ADP at 1 or 5 min. At 1 min, a reduced Rap1 activation was seen with TRAP-6, but this had attenuated at 5 min (Fig. 4, a and b). In contrast to ADP and TRAP-6, PMA induces a slow but normal GTP-binding to Rap1 in both patients and controls (seen at 5 min). Rap1 GTPγs loading revealed that Rap1 in the patient has no intrinsic defect. To prove that the p.G248W transition results in a reduced ability of CalDAG-GEFI to activate Rap1, we used HEK293T cells transfected with plasmids coding for

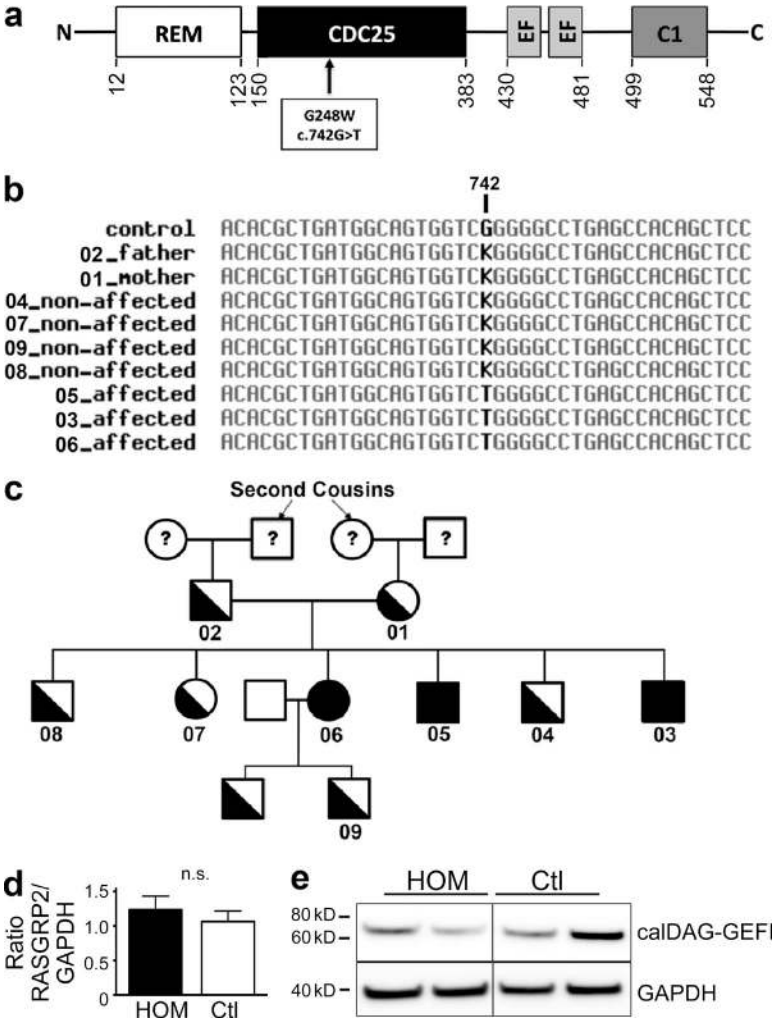

Figure 2. ***RASGRP2*** **gene mutation screening in family members and CalDAG-GEFI expression in platelets of the patients.** (a) CalDAG-GEFI primary structure showing the G248W substitution and the different structural domains: ras exchange motif (REM), catalytic domain (CDC25), calcium-binding EF hands (EF), and diacylglycerol-binding (C1). (b) Multiple alignment of genomic DNA sequence (Chr11: 64,494,383-64,512,928; National Center for Biotechnology Information Build 36) surrounding the putative disease-causing mutation (in bold). K is the IUPAC-IUB ambiguity code for G or T. (c) Family pedigree. Whole-exome sequencing was performed in #01, #02, #04, #05, and #06. Direct capillary sequencing confirmed the complete segregation of the p.G248W mutation. (d) Relative CalDAG-GEFI mRNA expression levels from homozygous (HOM) and healthy (Ctl) platelets. The relative amounts of *RASGRP2* mRNA were normalized to *GAPDH* mRNA levels. Data are mean ± SEM (Student's *t* test). (e) Representative Western blot for CalDAG-GEFI in platelet lysates from two homozygous (HOM) and two healthy subjects (Ctl). GAPDH expression was used as equal loading and electrophoretic transfer control.

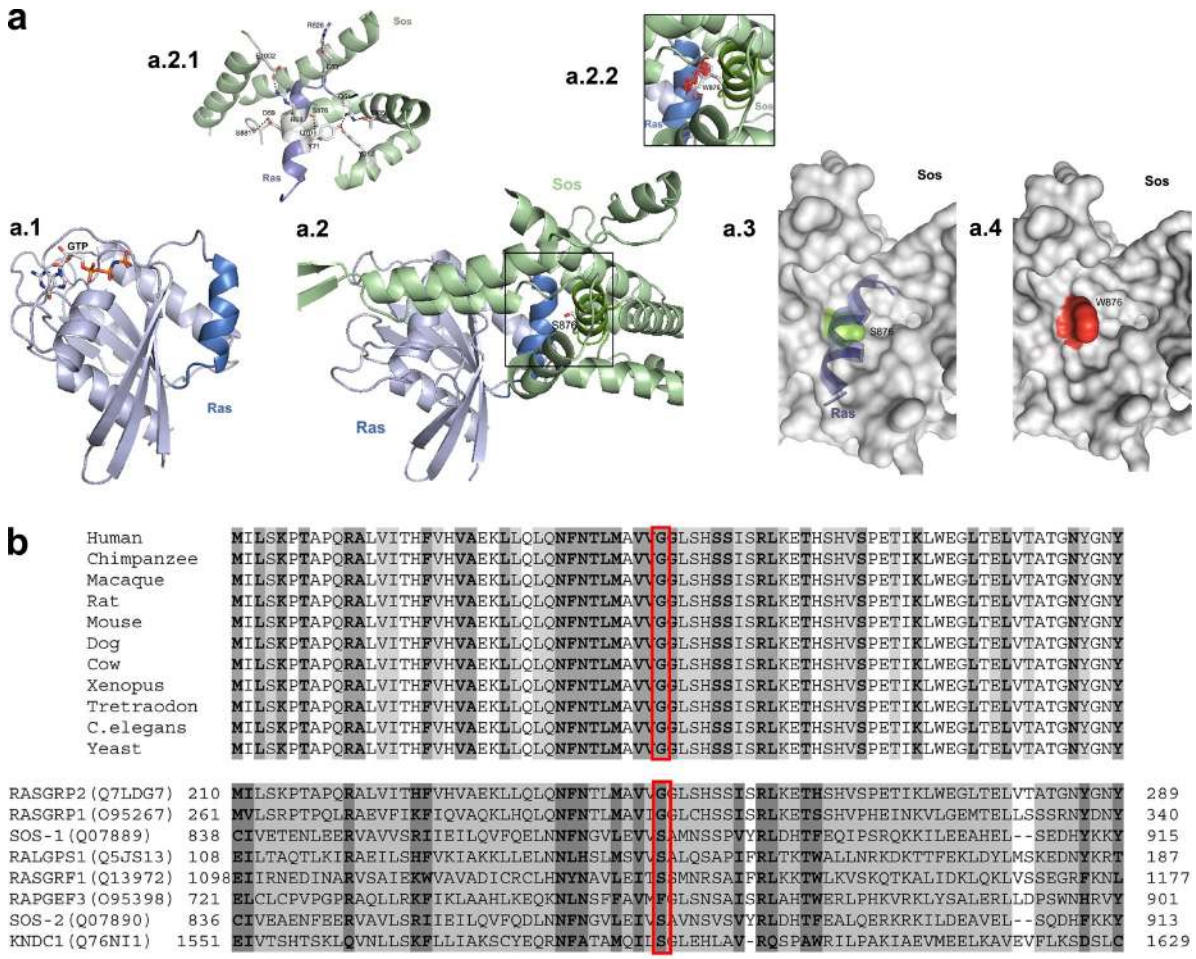

Figure 3. Predicted structural consequences on CalDAG-GEFI of the *RASGRP2* mutation. (a) SOS-2/Ha-ras protein sequence modeling. (a.1) Computer-drawn ribbon diagram of Ha-ras (light blue) and an analogue of GTP (sticks). (a.2) Ha-ras (light blue) in association with Sos-2 (pale green). The frame indicates the region of the tight interaction of Ha-ras with the CDC25 domain of the Sos-2 protein concerned by the mutated amino acid. (a.2.1) Amino acids (sticks) contributing to H-bonds (dotted lines) for the CDC25 domain of Sos-2 and its interaction with Ha-ras. The S876W mutation is shown in a small window (a.2.2) as a graphical stick representation; graphical "bumps" (red discs) indicate steric interactions caused by the S876W substitution. (a.3 and a.4) The CDC25 domain-forming cavity is depicted as a molecular surface. S876 (a.3) is colored in green. α-Helix of Ha-ras lying within the cavity is shown in blue. W876 forming protrusion (a.4) is colored in red. (b) Sequence alignment of RASGRP2 (SCR2 region) through species (orthologue; top), and through different members of their protein family in human (paralogue; bottom). The frame highlights the amino acids participating in the H-bonds.

Rap1 and either the normal or the mutated CalDAG-GEFI. In Rap1 and normal CalDAG-GEFI co-transfected cells, calcium ionophore stimulation triggers a significant Rap1 activation (Fig. 4 c). However, when cells are co-transfected with Rap1 and mutated CalDAG-GEFI, no increase in Rap1 activation is noticed. No detectable amount of endogenous CalDAG-GEFI was observable in HEK293T cells. Indeed, HEK293T cells transfected with Rap1 alone did not show any activation of Rap1 upon calcium ionophore stimulation. These results clearly demonstrate that the p.G248W mutation a strong impairment of CalDAG-GEFI activity.

In the absence of functional CalDAG-GEFI, platelet aggregation requires P2Y12 signaling

In CalDAG-GEFI–deficient mice, platelet aggregation mediated by the thrombin PAR receptor required co-signaling through the $G\alpha_i$-coupled P2Y12 receptor for ADP (Cifuni et al., 2008). Accordingly, pharmacologic inhibition of the P2Y12 receptor with 2-MesAMP in platelets from patients carrying the mutated form of *RASGRP2*, prevented the residual aggregation observed upon stimulation by low-dose (10 μM) but not high-dose (50 μM) TRAP-14 (Fig. 5 a).

Functional consequences of the p.G248W transition on platelet adhesion and spreading

Next, we tested ability of platelets from the patients to bind soluble and immobilized fibrinogen as compared with normal platelets. We observed a reduced binding of soluble fibrinogen to platelets from homozygous patients in the presence of ADP or TRAP-6 (Fig. 5 b), as well as a diminished adhesion to surface-bound fibrinogen in the absence of agonists (Fig. 5 d). PMA normalized fibrinogen binding and adhesion for the

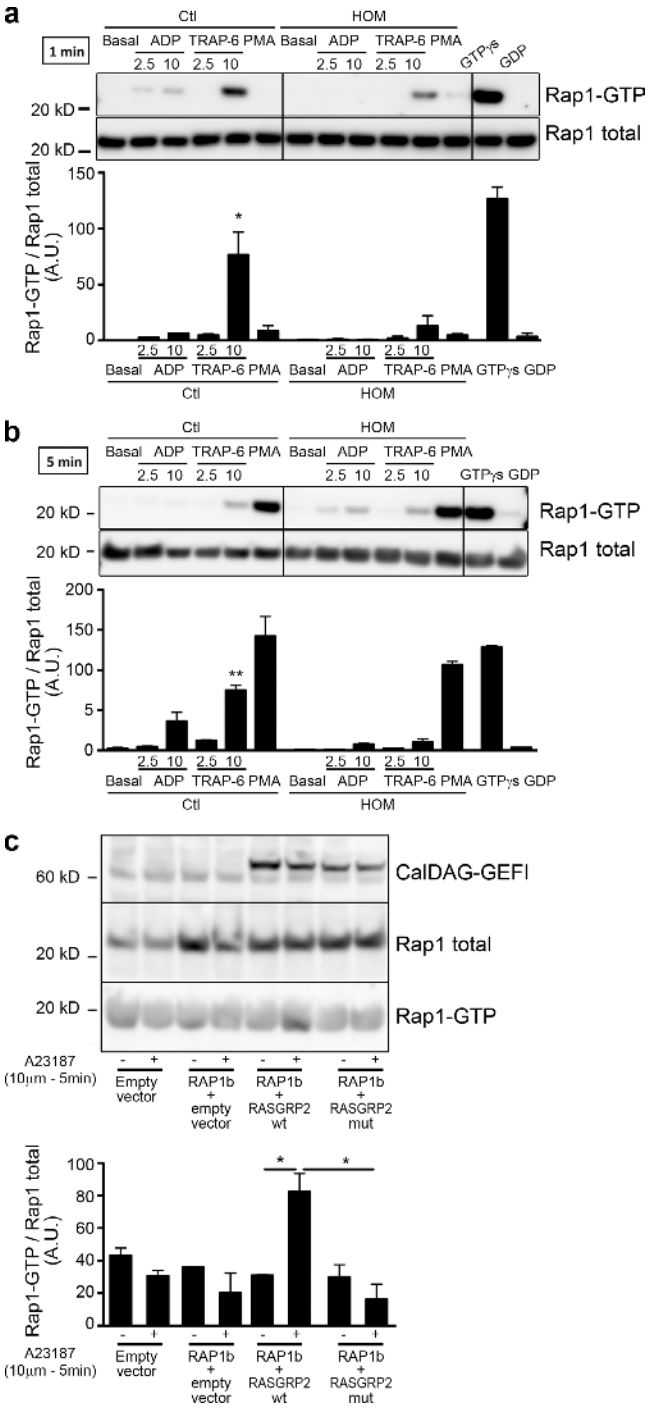

Figure 4. pG248W transition impairs CalDAG-GEFI's ability to activate Rap1. Activated Rap1 (Rap1-GTP) was detected in platelet lysates obtained from homozygous (HOM) and control (Ctl) subjects at 1 (a) and 5 min (b) after addition of ADP, TRAP-6, or PMA (150 nM). Incubation with GTP-γS and GDP were performed on platelet lysates from a homozygous patient. Presented results are representative of three independent experiments. Densitometry analysis shows the band density ratios of Rap1 GTP to total Rap1 as indicated in the panels below. Student's *t* test revealed significant differences between control subject and homozygous patient platelet preparation treated with corresponding agonists (*, P > 0.05; **, P > 0.001). Data are mean ± SEM; *n* = 3.

patients' platelets (Fig. 5, b and e). To unequivocally attribute this integrin activation defect to the p.G248W transition in CalDAG-GEFI, rescue experiments were performed with megakaryocytes from the patients and healthy individuals. These were obtained from differentiated $CD34^+$ cells transduced with a vector containing the EGFP and the wild-type form of *RASGRP2* sequences or the EGFP alone. The patient's cells infected with the vector containing only EGFP showed a defect in fibrinogen binding when stimulated by 10 and 50 μM TRAP-6 (Fig. 5 c), thereby confirming that the CALDAG-GEFI defect extended to megakaryocytes. Expression of the wild-type form of CalDAG-GEFI in the patient's megakaryocytes restored fibrinogen binding at a level observed in control megakaryocytes transduced with the vector containing EGFP alone. To test whether the mutation in *RASGRP2* affects platelet function under conditions that mimic arterial blood flow, we studied platelet adhesion and thrombus formation during perfusion over fibrillar collagen. The surface covered by platelets of homozygous patients was strongly reduced in comparison to controls all along the time course of the experiment (Fig. 5 f). Although there was no obvious defect in platelet aggregation (unpublished data), the adhesion kinetics were surprisingly altered for obligate heterozygous carrying a single mutated allele and, except at early time points, results were similar to those obtained for homozygous subjects (Fig. 5 f, right). When exposed to extracellular matrix protein, platelets undergo complex cytoskeletal rearrangements modifying their morphology leading to the increase of their surface area and spreading. During spreading, platelets sequentially form fingerlike filopodia and lamellipodial sheets. We tested whether the p.G248W transition in CalDAG-GEFI affects platelet spreading over immobilized fibrinogen. Platelets from patients exhibited a reduced number of filopodia and failed to form lamellipodia either when platelet on fibrinogen alone or in the presence of ADP (Fig. 6, a and b) and TRAP-6 (not depicted). Significantly, platelets of a heterozygous patient also showed a pronounced spreading defect with no lamellipodia formation; however, they were more prone to form filopodia upon activation compared with platelets from homozygous carriers. In contrast to aggregation, the presence of high doses of ADP and TRAP-6 only partially reversed the spreading defect, indicating that complete CalDAG-GEFI activity is required for full spreading. Nevertheless, normal spreading was obtained in the presence of PMA (Fig. 6 c).

(c) CalDAG-GEFI–dependent activation of Rap1 in HEK293T. Rap1 was co-transfected with either the empty vector or the mutated form of RASGRP2. After stimulation with calcium ionophore (10 μM, 5 min), cells were lysed and Rap1-GTP was pulled down. The representative blots of two independent experiments are shown. Densitometry analysis shows the band density ratios of Rap1 GTP to total Rap1 as indicated in the left panel. Student's *t* test revealed significant differences (*, P > 0.05). Data are mean ± SEM; *n* = 2.

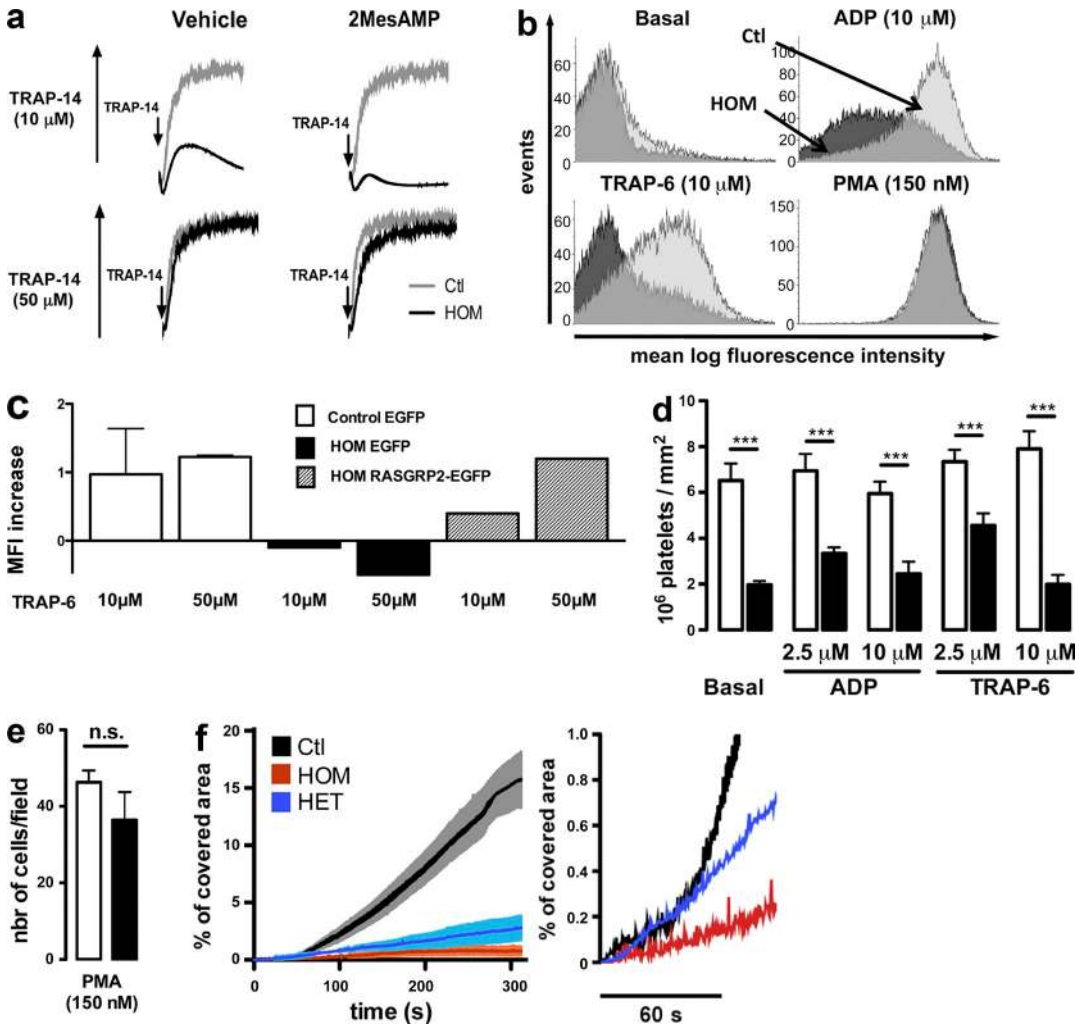

Figure 5. Evidence for CalDAG-GEFI bypassing pathways and defective platelet adhesion caused by the CalDAG-GEFI mutation. (a) Aggregation tracings from homozygous (HOM) and normal (Ctl) platelets with low- (top) or high-dose (bottom) TRAP-14 with or without the P2Y12 inhibitor 2MesAMP (100 μM). (b) FITC-labeled fibrinogen binding to platelets. Histograms are representative MFI of two independent experiments. (c) Alexa Fluor 647–labeled fibrinogen binding to megakaryocytes from a HOM patient and healthy controls ($n = 2$) transduced with RASGRP2-EGFP vector or EGFP vector control. On megakaryocytes, fibrinogen binding upon stimulation of cells in suspension by TRAP-6 (10 and 50 μM) was measured by flow cytometry. Results are expressed as MFI increase over the unstimulated state. (d) Static adhesion of platelets from homozygous ($n = 2$) and healthy ($n = 6$) subjects on fibrinogen (mean ± SEM 10^6 platelets/mm^2; Student's t test; ***, $P < 0.001$). (e) PMA-induced adhesion on fibrinogen of platelets from homozygous (filled bars; $n = 1$) and healthy (open bars; $n = 4$) subjects (mean ± SEM platelet per view field; Student's t test). (f) Adhesion under flow (750 s^{-1}) on collagen of calcein-AM–labeled platelets from a homozygous (HOM), a heterozygous (HET), or a healthy (Ctl) subject. Percentage of covered area was assessed over 300 s (left). The initial 60 s are magnified (right). Results are mean ± SEM; ($n = 3$ in each groups).

A defective activation of Rac1, but not Cdc42, correlates with the spreading defect observed in CalDAG-GEFI–mutated platelets

Rho GTPase family members Cdc42 and Rac1 are key regulators of platelet cytoskeleton dynamics (Aslan and McCarty, 2013). Furthermore, recent evidence supports cooperation between Rap1 and Rac1 (Stefanini et al., 2012). In view of this, we tested the effect of the mutation in CalDAG-GEFI on GTP-binding on Rac1 and Cdc42. The mutation in CalDAG-GEFI resulted in a strong reduction in Rac1 activation at 1 min after platelet stimulation with ADP and TRAP-6 (Fig. 6 d). This effect was more pronounced after TRAP-6 stimulation as compared with ADP. On the other hand, the p.G248W transition only moderately affected GTP-binding to Cdc42 (Fig. 6 e). These results may help explain the spreading defect observed in platelets from our patients.

The p.G248W transition in CalDAG-GEFI has little impact on leukocyte functions

Data obtained with CalDAG-GEFI–deficient mice suggest a role for CalDAG-GEFI in integrin-dependent and -independent leukocyte functions (Bergmeier et al., 2007; Carbo et al., 2010).

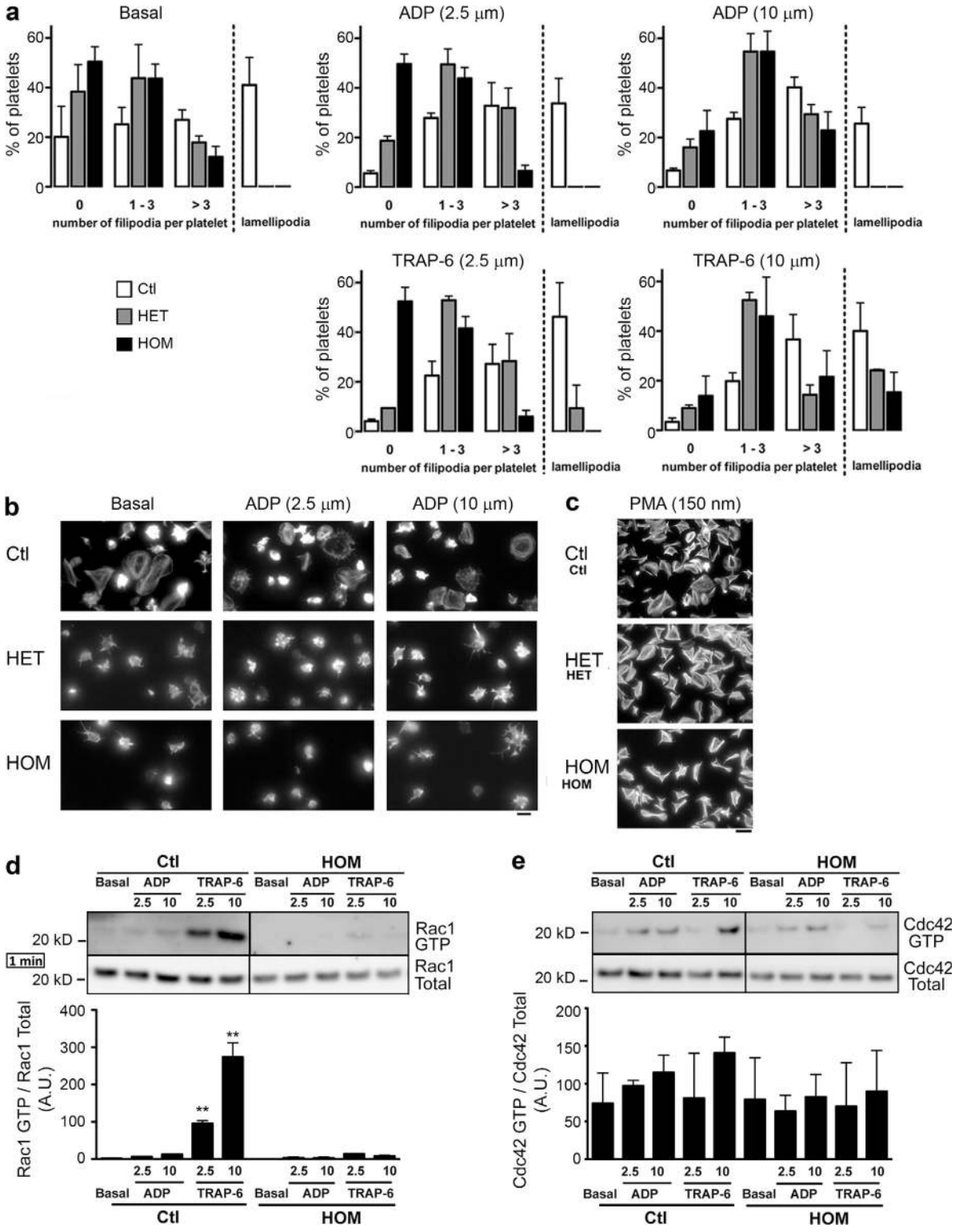

Figure 6. Incomplete platelet spreading results from the p.G248W transition in CalDAG-GEFI. (a) Platelet spreading over immobilized fibrinogen from homozygous (HOM), heterozygous (HET), or healthy (Ctl) subjects. Representative results from two separate experiments, expressed as means ± SEM of 5 different view fields (Chi-squared test; for Ctl vs. HOM and Ctl vs. HET, $P < 0.001$ in all tested conditions; for HOM vs. HET: $P < 0.001$ for ADP 2.5 μM and TRAP-6 2.5 μM, $P = 0.186$ at basal state, $P = 0.378$ for ADP 10 μM, and $P = 0.669$ for TRAP-6 10 μM). (b and c) Representative images of platelet spreading from homozygous (HOM), heterozygous (HET) or healthy (Ctl) subjects in the presence of ADP and PMA (scale bars are 4 μm and 20 μm for b and c, respectively). (d and e) GTP loading shown for Rac1 and Cdc42 for platelets of HOM and Ctl subjects for ADP or TRAP-6 stimulation for 1 min. Rep-

In our patients, the *RASGRP2* mutation is not associated with a clinically manifested immunodeficiency. Subnormal white blood cell counts were found in the three homozygotes (total, 12.28 ± 1.49 G/l; neutrophils, 8.89 ± 1.11 G/l; lymphocytes, 2.41 ± 0.48 G/l; monocytes, 0.36 ± 1.12). In contrast to data that we have previously obtained on LAD-III lymphocytes (Robert et al., 2011), the patients' lymphocytes showed only a minor defect in β2-integrin activation. Lymphocyte spreading on an ICAM-1–coated surface was not detectable in patients and was very limited for controls. Nonetheless, spreading occurred normally on anti-CD3 antibody and was potentiated to the same extent in patients and controls when ICAM-1 and anti-CD3 antibody were combined (unpublished data). Testing neutrophils from the patients revealed that the *RASGRP2* mutation was without effect on reactive oxygen species generation, adhesion, and chemotaxis, which clearly distinguishes the functional defect from the typical leukocyte dysfunction in LAD-III (Fig. 7 a). Using a more physiologically relevant model, we tested patients' neutrophil adhesion and transmigration on TNF-activated human umbilical vein endothelial cells (HUVEC). In this setting, neutrophil adhesion and transmigration is almost fully blocked by anti-CD11b/CD18 and anti–ICAM-1 antibodies (Gopalan et al., 2000). We did not observe any difference for neutrophils from homozygous patients and controls (Fig. 7 b).

DISCUSSION

We have identified for the first time a point mutation in *RASGRP2* in man associated with severe bleedings in three siblings. The reported mutation induces platelet dysfunction but spares leukocyte function. Significantly, αIIbβ3 integrin inside-out and outside-in signaling were strongly impaired. Activation of Rap1 and Rac1 were reduced, whereas GTP-binding to Cdc42 was only moderately affected. We have highlighted the presence of CalDAG-GEFI bypassing pathways dependent on PKC and ADP. Remarkably, the presence of only one normal allele is sufficient to prevent bleeding and to support normal platelet aggregation but not full platelet adhesion and spreading. Significantly, the ability of αIIbβ3 to bind fibrinogen was rescued when normal CALDAG-GEFI expression was induced in megakaryocytes cultured from $CD34^+$ cells of homozygous patients.

Whole exome sequencing is now a proven strategy for discovering the rare alleles underlying Mendelian inherited disorders. Our approach resulted in a list of only four candidate genes among which the *RASGRP2* gene stood out. *RASGRP2* encodes for CalDAG-GEFI, a GEF that regulates Rap1b activation, its prototypical substrate in platelets that modulates the affinity and avidity of the integrin αIIbβ3 (Bertoni et al., 2002; Eto et al., 2002; de Bruyn et al., 2003). The mutation described here is located in the sequence encoding SCR2 of CDC25 and was predicted by the PolyPhen-2 software to have functional consequences. Accordingly, the mutation causes the exchange of a small neutral amino acid with a large polar one, which predicts obstruction within the cavity of the GEF.

A splice-site mutation in *RASGRP2* resulting in the absence of CalDAG-GEFI was reported as the cause of a severe bleeding disorder (LAD-III; Pasvolsky et al., 2007) but this was later revised when defective kindlin-3 was unequivocally established to be responsible (Kuijpers et al., 2009). Clinical features of our patients differ from the reported LAD-III cases (Alon et al., 2003; Kuijpers et al., 2007, 2009; Malinin et al., 2009; Raaijmakers and Bos, 2009; Svensson et al., 2009; Jurk et al., 2010; McDowall et al., 2010; van de Vijver et al., 2012). Bleedings were milder and revealed later in infancy. Moreover, none of the affected members suffer from immune deficiency or wound healing problems which are hallmarks of LAD-III (Alon et al., 2003; Kuijpers et al., 2007, 2009; Malinin et al., 2009; Raaijmakers and Bos, 2009; Svensson et al., 2009; Jurk et al., 2010; McDowall et al., 2010; van de Vijver et al., 2012). In addition, kindlin-3 protein levels in platelets and the *FERMT3* gene sequence were normal in our patients. In agreement with the clinical presentation, the patients showed no defects in β2-mediated neutrophil functions. These results indicate that the mutation is in accordance with a more lineage-restricted expression of RasGRP family members within the hematopoietic system (Stone, 2011). Mutations in SCRs of *RASGRP2* were previously described in calves and dogs suffering bleeding disorders (Boudreaux et al., 2007a,b). Similarly, no immune deficiency has been reported in these species. However, a role for CalDAG-GEFI in leukocyte functions was suspected since silencing *RASGRP2* in human T cells in vitro, inhibits SDF-1α– and PMA–induced adhesion to ICAM-1 (Ghandour et al., 2007) and neutrophils from CalDAG-GEFI-deficient mice failed to adhere firmly to stimulated venules or to migrate into sites of inflammation (Bergmeier et al., 2007; Carbo et al., 2010; Stadtmann et al., 2011). One possible explanation for these discrepancies could be that the point mutation that we have described spares structural domains that might be important for leukocyte functions when compared with total CalDAG-GEFI deficiency in mouse knock-out models. Alternatively, other GEFs in human leukocytes could substitute for CalDAG-GEFI in Rap1 activation (Minato et al., 2007; Raaijmakers and Bos, 2009). Thus, it would be of great interest to study in detail the role of Rap1b in β-integrin–dependent human leukocyte functions in vivo.

Platelet aggregation responses in heterozygous patients did not differ from those obtained for healthy controls. For the homozygous carriers, aggregation results were similar to

resentative blots of three independent experiments. Densitometry analysis shows the band density ratios of Rac1 GTP to total Rac1 and Cdc42 GTP to total Cdc42 as indicated in the panels below. Student's *t* test revealed significant differences between control subject and homozygous patient platelet preparation treated with corresponding agonists (**, P > 0.001). Data are mean ± SEM; *n* = 3.

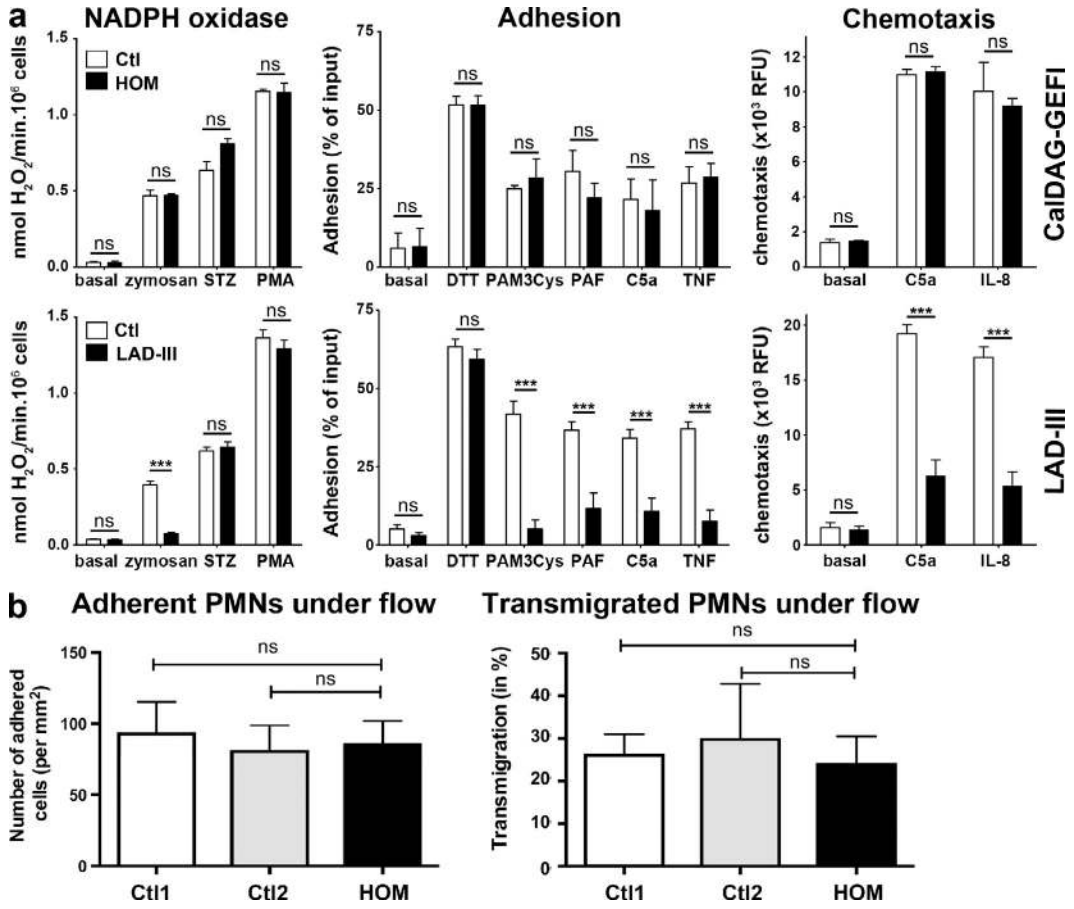

Figure 7. Function testing of neutrophils from a homozygous carrier of the *RASGRP2* mutation, a LAD-III patient, and control subjects. Neutrophils from a patient carrying homozygous *RASGRP2* mutation, a LAD-III patient, and control subjects were isolated from blood. (a) NADPH oxidase activity revealed as hydrogen peroxide production (nmol/min) in response to stimuli (left). Maximal activities were measured over 30 min of incubation; STZ, serum-treated zymosan; PAF, platelet activating factor; fMLP, formyl-Met-Leu-Phe. The middle panel shows neutrophil adhesion to fibronectin upon activation. The right panel shows neutrophil chemotaxis. Results were expressed as relative fluorescence unit (NADPH oxidase activity data were obtained from 18 independent experiments; adhesion data were from 8–13 independent tests and chemotaxis from 7–9). Data are expressed as means ± SEM (Student's *t* test; ***, $P < 0.001$). (b) Neutrophils adhesion (left) and transmigration (right) on TNF-activated HUVECs under flow conditions (2 dynes/cm^2). Control neutrophils originate from either local healthy individual (Ctl1) or from blood shipped in the same manner as the patients' samples (Ctl2). Results are expressed as mean ± SEM; $n = 3$.

those previously obtained in cattle and dogs carrying homozygous mutations in the SCR domains and in CalDAG-GEFI-deficient mice in agreement with the comparison through species (Boudreaux et al., 2007a). Maximal aggregation in response to all tested doses of ADP or low doses of any other agonists was reduced. In addition, we observed a concordant reduction of Rap1 activation. In contrast, PMA induces the same extent of aggregation as well as adhesion, spreading and Rap1 activation in both patients and controls highlighting, as in mice (Cifuni et al., 2008), the existence of a PKC-dependent Rap1 activation pathway that is independent of CalDAG-GEFI.

Thrombin-induced aggregation in the absence of CalDAG-GEFI in mice required co-signaling through the $G\alpha_i$-coupled receptor for ADP, P2Y12 (Cifuni et al., 2008). We also confirmed the presence of a CalDAG-GEFI-independent but ADP-dependent pathway after stimulation through PAR-1. In addition, pharmacologic inhibition of the P2Y12 receptor prevented the residual aggregation in platelets from homozygous carriers stimulated by low dose of TRAP but not by a high dose. Surprisingly, although aggregation was completely abolished in CalDAG-GEFI–deficient mice at a high dose of ADP (50 μM; Crittenden et al., 2004), partial aggregation and fibrinogen binding were found in homozygous patients at 10–50 μM ADP. In addition, no GTP-binding to Rap1 was observed in platelets from homozygotes stimulated with exogenous ADP (2.5 and 10 μM). These results indicate that CalDAG-GEFI is most probably the only Rap1-activating GEF triggered by exogenous ADP in human platelets and highlight the existence, in human platelets, of a pathway triggered by ADP controlling inside-out signaling that is independent of both the CalDAG-GEFI SCR2 domain and Rap1. In agreement, ADP-induced aggregation is attenuated but not totally absent in Rap1b-null platelets (Chrzanowska-Wodnicka

et al., 2005) and low doses of ADP restore normal aggregation induced by thrombin or collagen in platelets from these animals (Zhang et al., 2011). Altogether, these data strongly support the presence in human platelets of alternative pathways for integrin activation that do not require CalDAG-GEFI SCR2 domain and Rap1.

In addition to platelet aggregation, we examined platelet spreading, a complex phenomenon dependent on signaling downstream from integrin engagement. As compared with control platelets, those from subjects with the mutated form of CalDAG-GEFI (either single or double dose mutated allele) exhibited a decreased number of filopodia and never formed lamellipodia when plated on solid-phase fibrinogen, regardless of the stimulation conditions. Accordingly, CalDAG-GEFI–deficient mice showed a decreased mean area of adherent platelets when spreading over monomeric collagen (Bernardi et al., 2006) and CalDAG-GEFI/P2Y12 double knock-out mice failed to form lamellipodia despite filopodia forming on this surface (Stefanini et al., 2012).

Under arterial flow and over fibrillar collagen, the surface covered by platelets of homozygous or heterozygous patients was strongly reduced in comparison to controls. It has been shown that CalDAG-GEFI knock-out platelets have a reduced ability to adhere to fibrillar collagen and are resistant to collagen-induced thrombosis in vivo (Crittenden et al., 2004). Furthermore, thrombosis was virtually abolished in arterioles and arteries of CalDAG-GEFI–deficient mice (Stolla et al., 2011a). Intriguingly and different to the platelet aggregation results, exploration of obligate heterozygous carrying a single mutated allele revealed pronounced defects in adhesion under flow and spreading. Our results suggest that partial inhibition of the SCR2 of the CDC25 catalytic domain could prevent thrombosis without affecting physiological hemostasis. Interestingly, Stolla et al. (2011b) reported that, in mice, the absence in circulating platelets of another domain of CalDAG-GEFI, the C1-like domain, also led to protection from thrombus formation at arterial flow conditions whereas it only marginally increased blood loss.

In conclusion, we report the first case of a human *RASGRP2* mutation causing severe bleeding. We observe a functional deficiency primarily in platelets, and only minor effect on leukocytes. Our results indicate a selective defect in platelet-signaling pathways mainly observable at low dose of agonists. The CalDAG-GEFI dysfunction can be bypassed at high doses of agonists and platelet spreading is more severely affected than platelet aggregation. Significantly, the presence of a single normal allele is sufficient to prevent bleeding, to support normal aggregation but does not correct platelet adhesion under flow or spreading. This makes partial inhibition of the CalDAG-GEFI catalytic domain an interesting therapeutic target to prevent thrombosis without causing bleeding.

MATERIALS AND METHODS

Experiments. Investigations were performed in accordance with the Declaration of Helsinki. Written informed consent was obtained from the patients and healthy individuals.

Exome sequencing. The sequencing of the whole exome was performed on five subjects: the index case (individual 05), his two parents (individuals 01 and 02), an affected sister (individual 06), and an unaffected brother (individual 04). Exome sequencing was performed on genomic DNA extracted from saliva (Oragen DNA/saliva kit; DNA Genotek). DNA concentration was measured using Quant-iT PicoGreen dsDNA (Life Technologies).

One microgram of the diluted Genomic DNA was sheared with a Bioruptor instrument to obtain fragment sizes ∼200–300 bp using the following protocol: Low Power, 15 ON/OFF cycles (30 s each) with a rapid spin after 7 cycles. An adaptor-ligated library was prepared with the TruSeq DNA Sample Preparation kit (Illumina) according to the TruSeq DNA Sample Preparation protocol. An adaptor index specific to each sample was added during the "Ligate Adapters" step to allow multiplexing during the sequencing process. The resulting library was then validated on a high sensitivity DNA chip (Agilent) and quantified by Quant-iT dsDNA Assay kit_broad range (Life Technologies). Samples were then pooled using 500 ng of each index-specific DNA sample. The resulting pools then underwent exome capture with the Truseq Exome Enrichment kit (Illumina). The enriched library was validated and quantified on a high sensitivity DNA chip (Agilent). 7 pmol of each enriched library was loaded on a TruSeq Flowcell v1.5. After a clusterisation procedure performed with the TruSeq PE Cluster kit v2.5 (Illumina) on an Illumina cBot instrument, a 2 × 75 paired-end sequencing was performed on the Illumina HiSeq2000 instrument using a Truseq SBS–HS (200 cycles) kit (Illumina).

Sequenced data were aligned to the human genome reference sequencing hg19 build using the Consensus Assessment of Sequence and VAriation (CASAVA) software (http://www.illumina.com/software/genome_analyzer_software.ilmn). PCR and optical duplicates were discarded, as well as non-paired reads and reads with low-quality mapping (Q-score <20). The mean percentage of duplicate reads due to PCR or optical artifacts was 26% in our sequenced dataset. After removing these duplicates, ∼32.7 million uniquely mapped reads were obtained for each sample, with 80% of bases covered to at least 10X.

Variant calling was performed using the samtools program (Li et al., 2009) while the ANNOVAR software (Wang et al., 2010) was used to annotate the identified variants. Variants with low coverage (<10X) in affected individuals were discarded from the analysis.

Sequencing validation and genotyping. The presence/absence of the mutated form was confirmed in all family members by direct sequencing using Big Dye Terminator kit (Life Technologies). DNA was extracted from blood by a salting out procedure (Miller et al., 1988) and amplified by PCR using the following forward (A0665_F) and reverse (A0666_R) primers: A0665_F 5′-CATCACACACTTTGTCCACG-3′, A0666_R 5′-TCAAATGAGGACAGCTGTGC-3′. Sequencing reactions were done on both strands using forward and reverse primers, according to the supplier protocol, and ran on an ABI 3130xl Genetic Analyzer. Sequences analysis was done using Chromas X software, and aligned using Multalign (http://multalin.toulouse.inra.fr/multalin/).

RT-PCR. Total RNA was extracted from blood collected on TempusTM Blood RNA tubes (Life Technologies), and extracted using TempusTM Spin RNA isolation kit (Life Technologies). Reverse transcription was performed using M-MLVI reverse transcription (Life Technologies). Reactions, amplifications, and readings were performed on a LC480 type II instrument (Roche), using a standard SYBR Green preestablished amplification program, and analyzed using the Advanced Relative Quantification method. The following primer sequences were used for RT-PCR: RASGRP2 forward (A0540b_F) 5′-GCATGTTCCTCATGATGCAC-3′ and reverse (A0541_R) 5′-GAAGGCGGAGATCCAGTACC-3′; GAPDH forward 5′-AGCCACATCGCTCAGACAC-3′ and reverse 5′-GCCCAATACGACCAAATCC-3′. Expression is displayed as the percentage of RASGRP2/GAPDH relative expression ratio to a healthy control sample ratio.

Protein sequence modeling. Models were obtained using the PyMol Molecular Graphics System, version 1.3, and 5p21 and 1bkd Protein Data

Bank files for crystal structure of Ha-ras complexed with GTP and Ha-ras complexed with Sos-2, respectively. The amino acid change is rotamer incorporated from the Dunbrack Backbone library with the maximum probability.

Platelet preparation. PRP and washed platelets were prepared as previously described (Miller et al., 1988). Washed platelets were resuspended in Tyrode's buffer (138 mM NaCl, 2.7 mM KCl, 12 mM $NaHCO_3$, 0.4 mM NaH_2PO_4, 1 mM $MgCl_2$, 2 mM $CaCl_2$, 5 mM Hepes, 3.5 mg/ml HSA, and 5.5 mM glucose, pH 7.3) supplemented with 0.02 U/ml apyrase. Studies were performed within 6 h after blood collection.

Flow cytometry. Diluted PRP (0.25×10^8 platelets/ml) was gently mixed with antibodies against CD41/CD61 (clone P2), CD42b/CD42d/CD42a (clone SZ1), CD62P (clone CLB-Thromb/6), CD63 (clone CLB-grad12; Beckman Coulter), or antibody directed against the active form of αIIbβ3 (clone PAC-1; BD). Fibrinogen binding was measured on PRP (2×10^8 plt/ml) incubated with Alexa Fluor 488–labeled human fibrinogen (Life Technologies). Scatter signals and fluorescence intensity were analyzed using a FC500 flow cytometer (Beckman Coulter).

Platelet aggregation. Diluted PRP (3×10^8 plt/ml in platelet-poor plasma) was placed in an aggregometer cuvette at 37°C and stirred. Agonists were added (ADP, arachidonic acid, and epinephrine were purchased from Helena Laboratories; collagen was purchased from Bio/Data Corporation; TRAP-14 was obtained from Polypeptide group; and ristocetin was obtained from Stago) at concentrations given in the text. Light transmission was recorded on an APACT 4004 optical aggregation system (Labor Bio-Medical Technologies GmbH).

Platelet adhesion and spreading under static conditions. Washed platelets (10^7 platelets/ml in Tyrode's buffer containing 1 mM $MnCl_2$ and 1 mM $CaCl_2$) were added to human fibrinogen-coated glass coverslips (100 µg/ml; LFB) for 45 min at 37°C in the presence or absence of ADP (2.5 µM and 5 µM), TRAP-6 (2.5 µM and 5 µM) or PMA (150 nM). Rinsed coverslips were then fixed in 1% paraformaldehyde for 15 min at room temperature. Spread platelets were incubated with 1% saponin in PBS containing 5 µM phalloidin. Platelets were visualized with an AxioImager M1 microscope (100× oil objective). Digital images were recorded using an Axiocam MRm camera (Carl Zeiss, Inc.) and analyzed off-line using ImageJ (National Institutes of Health) software. Images of adherent platelets were used to manually count five different fields of view for each subject. Spreading was evaluated by quantifying the number of filopodia per platelet (0, 1–3, >3) and the percent of platelets forming lamellipodia at basal state and upon ADP (2.5 and 10 µM) and TRAP-6 (2.5 and 10 µM) stimulation.

Platelet adhesion under flow conditions. Vena8 Fluoro+ biochips (Cellix) were coated with 100 µg/ml bovine type I collagen (Life Technologies). Platelets were labeled in PRP with 1 µg/ml calcein for 30 min. Reconstituted whole blood containing 100 µM D-Phe-L-Pro-L-Arg chloromethyl ketone (PPACK) and 2.5 mM $CaCl_2$ was injected into the channels using a syringe pump at 750 s^{-1}. Platelet adhesion was visualized with an IX71 inverted microscope equipped with a XC-50 digital color camera (Olympus). Images were recorded for 300 s and analyzed off-line using ImageJ software. The kinetics of thrombus formation was evaluated by plotting the integrated fluorescence intensity of all pixels in the image, regardless of their intensity, as a function of time. The experiment was repeated four times for each blood sample.

Immunoblot analysis. PRP was centrifuged at 1,000 g for 5 min. Platelets were lysed with 10 mM Tris-HCl, 150 mM NaCl, 3 mM EDTA, 6 mM N-Ethylmaleimide, and 2.5% sodium dodecyl sulfate (SDS), pH 7.00, containing Pefabloc SC (Sigma-Aldrich). Total protein from the cell lysates was assayed using the Bicinchoninic Acid kit (Sigma-Aldrich). Samples (50 µg protein) were separated by SDS-PAGE and transferred onto a polyvinylidene difluoride membrane. Individual proteins were detected with antibodies against kindlin-3 (URP2; Abcam), CalDAG-GEFI (RASGRP2; Abcam), and human Glyceraldehyde-3-Phosphate Dehydrogenase and GAPDH (clone 6C5; Millipore). Secondary antibodies were either goat anti–rabbit or anti–mouse horseradish peroxidase coupled (Bio-Rad Laboratories). Proteins were visualized by chemiluminescence.

Small-GTPase activation assays. Rap1, Rac1, and Cdc42 activation were determined using commercially available kits (Millipore) by pull-down assay followed by standard Western blotting procedures as recommended by the manufacturer. Washed platelets (3×10^8 platelets/ml) were stimulated for 1 or 5 min in nonstirring conditions at 37°C with ADP (2.5 or 10 µM), TRAP-6 (2.5 or 10 µM), or PMA (150 nM). Reactions were stopped with ice-cold 2x Rap1 or Rac1/Cdc42 lysis buffer complemented with protease inhibitor cocktail (Roche) and phosphatase inhibition cocktail (Sigma-Aldrich). Cell lysis was completed on ice for 15 min. The cell lysates were incubated sequentially, for 45 min with PAK-1-PBD beads and RalGDS-RBD beads to pull-down Rac1/Cdc42-GTP and Rap1-GTP, respectively. Washed pellets were solubilized in sample buffer. Individual proteins were detected with a rabbit polyclonal antibody against Rap1 (Millipore), monoclonal antibodies against Rac1 (clone 23A8; Millipore), or Cdc42 (clone M152; Abcam). Secondary antibodies were either a goat anti–rabbit or anti–mouse horseradish peroxidase coupled (Bio-Rad Laboratories). Proteins were visualized by chemiluminescence. GTPγS and GDP were incubated with homozygous platelet lysates before pull-down assays to detect total activatable Rap1. No Rap1-intrinsic defect was revealed. Incubation of homozygous platelet lysates with GDP served as negative Rap1 activation control. Total Rap1 levels were detected in whole platelet lysates. Detections of total Rap1 and Rap1-GTP were performed using anti-Rap1 polyclonal antibody.

HEK293T cells co-transfection. 1,820-bp sequences of the native form of human *RASGRP2* (NM_133819.1) and the mutated form were synthetized (ProteoGenix). The DNA sequences were subcloned into the pCDNA3.1 vector. HEK293T cells were transfected with Rap1 (1.35 µg) and CalDAF-GEFI (150 ng) using PolyJet transfection reagent (SignaGen Laboratories). 36 h after transfection, cells were washed and then stimulated with calcium ionophore (10 µM) for 5 min before cell lysis. 50 µl of whole lysate solution was collected for total protein analysis and Rap1-GTP was precipitated using RalGDS-RBD beads as described above.

Lentiviral vector cloning and viral particle production. The 1,820-bp sequence of the native form of human *RASGRP2* (NM_133819.1) with four restriction sites (HindIII and MluI upstream; NheI and XhoI downstream) and a Kozak sequence was synthetized (ProteoGenix). The DNA was subcloned into a third generation of HIV-derived lentiviral vector (pRRLsin-PGK-IRES2-eGFP-WPRE; Généthon). This vector contains an HIV central polypurine tract, a self-inactivating deletion in the U3 region of the 3′LTR (ΔU3), the eGFP downstream of the encephalomyocarditis virus IRES, and the woodchuck hepatitis virus posttranscriptional regulatory element (WPRE).

Lentiviral stocks were prepared as previously described (Naldini et al., 1996; Raslova et al., 2004) with slight modifications. In brief, viral particles were prepared by transient co-transfection in human 293T cells of three plasmids (SIN transfer vector plasmid, with or without *RASGRP2* sequence, the packaging plasmid pCMVΔ R8.74, and the VSV-G protein envelope plasmid pMD.G). Viral stocks were stored at −80°C, and concentrations of viral particles were normalized according to the p24 (HIV-1 capsid protein) content of supernatants.

Cell transduction and in vitro growth of megakaryocytes from CD34$^+$ cells. $CD34^+$ cells were isolated from 80 ml of peripheral blood using CD34 magnetic beads (Miltenyi Biotec). Cells (10^5) were suspended in 100 µl of serum-free medium containing lentiviral particles (125 ng of viral p24/100 µl). After 12 h, a second infection was performed and the cells were

incubated 48 h. Cells were then washed and cultured in serum-free medium supplemented with the human cytokines: TPO (100 ng/ml) and SCF (250 ng/ml) for 14 d.

Flow-cytometric analysis of fibrinogen binding to transfected megakaryocytes. Fibrinogen binding was assessed using Alexa Fluor 647–labeled fibrinogen (Life Technologies) in the presence or absence of TRAP-6 (10 or 50 μM) and analyzed on an Accuri C6 cytometer.

Neutrophil NADPH oxidase activity, migration, and adhesion. Blood cells were fractionated by density gradient centrifugation over isotonic Percoll with a specific gravity of 1.076 g/ml (2,000 rpm, 18 min, 25°C). The interphase, containing the mononuclear cells, was removed. The pellet fraction, containing both erythrocytes and granulocytes, was treated for 10 min with ice-cold isotonic NHCI solution (155 mM NHCI, 10 mM KHCO, 0.1 mM EDTA, pH 7.4) to lyse the erythrocytes. Cells were centrifuged in the cold (1,200 rpm, 4 min), and residual erythrocytes were lysed for 3 min more. The remaining granulocytes were washed twice in PBS containing human serum albumin (HSA; 0.5% wt/vol). Granulocytes were resuspended in the incubation medium at a final concentration of $5 \times l0^6$ cells/ml and held at room temperature for functional studies. Neutrophils were >95% pure.

NADPH-oxidase activity. NADPH-oxidase activity was assessed as hydrogen peroxide release determined by an Amplex Red kit (Molecular Probes). Neutrophils (0.25×10^6/ml) were stimulated with platelet-activating factor (PAF) and Formyl-Methionyl-Leucyl-Phenylalanine (fMLP; both 1 μM, added simultaneously) and 1 mg/ml serum treated Zymosan STZ, or 100 ng/ml PMA in the presence of Amplex Red (0.5 μM) and horseradish peroxidase (1 U/ml). Fluorescence was measured at 30-s intervals for 20 min with the HTS7000+ plate reader. Maximal slope of H_2O_2 release was assessed over a 2-min interval. Using unopsonized zymosan, the same steps and procedures were followed, but fluorescence was measured for 60 min at similar 30-s intervals. Maximal slope of H_2O_2 release was assessed over a 2-min interval.

Chemotaxis. Chemotaxis of purified neutrophils was assessed by means of FluoroBlok inserts (Falcon; BD). Cells (5×10^6/ml) were labeled with calcein-AM (1 μM final concentration; Molecular Probes) for 30 min at 37°C, washed twice, and resuspended in Hepes buffer at a concentration of 2×10^6/ml. Chemoattractant solution (PAF, IL-8, and C5a, all at 10 nM; Sigma-Aldrich) or medium alone (0.8 ml/well) was placed in a 24-well plate, and 0.3-ml cell suspension was delivered to the inserts (3-μm pore size) and placed in the 24-well plate. Cell migration was assessed by measuring fluorescence in the lower compartment at 2.5-min intervals for 45 min with the HTS7000+ plate reader (Perkin Elmer) at an excitation wavelength of 485 nm and emission wavelength of 535 nm. Maximal slope of migration was estimated over a 10-min interval.

Adhesion. Adhesion was determined in 96-well MaxiSorp plates (Nunc), precoated or not with human plasma-derived fibronectin for 60 min at room temperature. Calcein-labeled cells (100 μl; 2×10^6/ml) were pipetted in the 96-well plate, and cells were stimulated with 25 μl solvent with PAF (final concentration, 1 μM), TNF (final concentration, 10 ng/ml), PMA (final concentration, 100 ng/ml), C5a (final concentration, 10 nM), fMLP (final concentration, 1 μM), PAM3Cys (final concentration, 20 μg/ml), LBP/LPS (20 ng/ml, LPS isolated from *E. coli* strain 055:B5; Sigma-Aldrich; LBP 50 ng/ml; R&D Systems), DTT (final concentration, 1 mM), or granulocyte colony-stimulating factor (GCSF; final concentration, 20 ng/ml) as stimulus. Plates were incubated for 30 min at 37°C. Thereafter, the plates were washed three times with PBS at room temperature. Adherent cells were lysed with 125 μl H_2O, containing 0.5% (wt/vol) Triton X-100 (10 min, room temperature). Fluorescence was measured with the HTS7000+ plate reader at an excitation wavelength of 485 nm and emission wavelength of 535 nm. Adhesion was determined as a percentage of total cell input (2×10^6/ml).

Statistical analysis. All the experiments reported in this study were repeated at least three times, and comparable results were obtained. The blots reported in the figures are representative images. Analysis of band intensity was performed by computer-assisted densitometric scanning using ImageJ software. Statistical analysis was performed with the Student's *t* test. The χ^2 test was used to test for distributional differences between controls and patients.

We thank Anton Tool and Laura Gutierrez for the neutrophil experiments and Monique Verdier for performing the Western blots.

Bioinformatic analyses benefitted from the C2BIG computing center funded by the Fondation pour la Recherche Médicale and the Région Ile de France. The Post-Genomic Platform of the Pitié-Salpêtrière (P3S) Hospital was supported by a grant from the Région Île-de-France.

The authors declare no competing financial interests.

Submitted: 6 March 2013
Accepted: 5 June 2014

REFERENCES

Alon, R., M. Aker, S. Feigelson, M. Sokolovsky-Eisenberg, D.E. Staunton, G. Cinamon, V. Grabovsky, R. Shamri, and A. Etzioni. 2003. A novel genetic leukocyte adhesion deficiency in subsecond triggering of integrin avidity by endothelial chemokines results in impaired leukocyte arrest on vascular endothelium under shear flow. *Blood*. 101:4437–4445. http://dx.doi.org/10.1182/blood-2002-11-3427

Aslan, J.E., and O.J. McCarty. 2013. Rho GTPases in platelet function. *J. Thromb. Haemost*. 11:35–46. http://dx.doi.org/10.1111/jth.12051

Bergmeier, W., T. Goerge, H.W. Wang, J.R. Crittenden, A.C. Baldwin, S.M. Cifuni, D.E. Housman, A.M. Graybiel, and D.D. Wagner. 2007. Mice lacking the signaling molecule CalDAG-GEFI represent a model for leukocyte adhesion deficiency type III. *J. Clin. Invest*. 117:1699–1707. http://dx.doi.org/10.1172/JCI30575

Bernardi, B., G.F. Guidetti, F. Campus, J.R. Crittenden, A.M. Graybiel, C. Balduini, and M. Torti. 2006. The small GTPase Rap1b regulates the cross talk between platelet integrin alpha2beta1 and integrin alphaIIb-beta3. *Blood*. 107:2728–2735. http://dx.doi.org/10.1182/blood-2005-07-3023

Bertoni, A., S. Tadokoro, K. Eto, N. Pampori, L.V. Parise, G.C. White, and S.J. Shattil. 2002. Relationships between Rap1b, affinity modulation of integrin alpha IIbbeta 3, and the actin cytoskeleton. *J. Biol. Chem*. 277:25715–25721. http://dx.doi.org/10.1074/jbc.M202791200

Boriack-Sjodin, P.A., S.M. Margarit, D. Bar-Sagi, and J. Kuriyan. 1998. The structural basis of the activation of Ras by Sos. *Nature*. 394:337–343. http://dx.doi.org/10.1038/28548

Boudreaux, M.K., J.L. Catalfamo, and M. Klok. 2007a. Calcium-diacylglycerol guanine nucleotide exchange factor I gene mutations associated with loss of function in canine platelets. *Transl. Res.* 150:81–92. http://dx.doi.org/10.1016/j.trsl.2007.03.006

Boudreaux, M.K., S.M. Schmutz, and P.S. French. 2007b. Calcium diacylglycerol guanine nucleotide exchange factor I (CalDAG-GEFI) gene mutations in a thrombopathic Simmental calf. *Vet. Pathol*. 44:932–935. http://dx.doi.org/10.1354/vp.44-6-932

Carbo, C., D. Duerschmied, T. Goerge, H. Hattori, J. Sakai, S.M. Cifuni, G.C. White II, M. Chrzanowska-Wodnicka, H.R. Luo, and D.D. Wagner. 2010. Integrin-independent role of CalDAG-GEFI in neutrophil chemotaxis. *J. Leukoc. Biol*. 88:313–319.

Chrzanowska-Wodnicka, M., S.S. Smyth, S.M. Schoenwaelder, T.H. Fischer, and G.C. White II. 2005. Rap1b is required for normal platelet function and hemostasis in mice. *J. Clin. Invest*. 115:680–687. http://dx.doi.org/10.1172/JCI22973

Cifuni, S.M., D.D. Wagner, and W. Bergmeier. 2008. CalDAG-GEFI and protein kinase C represent alternative pathways leading to activation of integrin alphaIIbbeta3 in platelets. *Blood*. 112:1696–1703. http://dx.doi.org/10.1182/blood-2008-02-139733

Crittenden, J.R., W. Bergmeier, Y. Zhang, C.L. Piffath, Y. Liang, D.D. Wagner, D.E. Housman, and A.M. Graybiel. 2004. CalDAG-GEFI integrates signaling for platelet aggregation and thrombus formation. *Nat. Med*. 10:982–986. http://dx.doi.org/10.1038/nm1098

de Bruyn, K.M., F.J. Zwartkruis, J. de Rooij, J.W. Akkerman, and J.L. Bos. 2003. The small GTPase Rap1 is activated by turbulence and is involved in integrin [alpha]IIb[beta]3-mediated cell adhesion in human megakaryocytes. *J. Biol. Chem.* 278:22412–22417. http://dx.doi.org/10.1074/jbc.M212036200

Eto, K., R. Murphy, S.W. Kerrigan, A. Bertoni, H. Stuhlmann, T. Nakano, A.D. Leavitt, and S.J. Shattil. 2002. Megakaryocytes derived from embryonic stem cells implicate CalDAG-GEFI in integrin signaling. *Proc. Natl. Acad. Sci. USA.* 99:12819–12824. http://dx.doi.org/10.1073/pnas.202380099

Ghandour, H., X. Cullere, A. Alvarez, F.W. Luscinskas, and T.N. Mayadas. 2007. Essential role for Rap1 GTPase and its guanine exchange factor CalDAG-GEFI in LFA-1 but not VLA-4 integrin mediated human T-cell adhesion. *Blood.* 110:3682–3690. http://dx.doi.org/10.1182/blood-2007-03-077628

Gopalan, P.K., A.R. Burns, S.I. Simon, S. Sparks, L.V. McIntire, and C.W. Smith. 2000. Preferential sites for stationary adhesion of neutrophils to cytokine-stimulated HUVEC under flow conditions. *J. Leukoc. Biol.* 68:47–57.

Hemker, H.C., R. Al Dieri, E. De Smedt, and S. Béguin. 2006. Thrombin generation, a function test of the haemostatic-thrombotic system. *Thromb. Haemost.* 96:553–561.

Jurk, K., A.S. Schulz, B.E. Kehrel, D. Räpple, H. Schulze, D. Möbest, W.W. Friedrich, H. Omran, E. Deak, R. Henschler, et al. 2010. Novel integrin-dependent platelet malfunction in siblings with leukocyte adhesion deficiency-III (LAD-III) caused by a point mutation in FERMT3. *Thromb. Haemost.* 103:1053–1064. http://dx.doi.org/10.1160/TH09-10-0689

Kawasaki, H., G.M. Springett, S. Toki, J.J. Canales, P. Harlan, J.P. Blumenstiel, E.J. Chen, I.A. Bany, N. Mochizuki, A. Ashbacher, et al. 1998. A Rap guanine nucleotide exchange factor enriched highly in the basal ganglia. *Proc. Natl. Acad. Sci. USA.* 95:13278–13283. http://dx.doi.org/10.1073/pnas.95.22.13278

Kuijpers, T.W., R. van Bruggen, N. Kamerbeek, A.T. Tool, G. Hicsonmez, A. Gurgey, A. Karow, A.J. Verhoeven, K. Seeger, O. Sanal, et al. 2007. Natural history and early diagnosis of LAD-1/variant syndrome. *Blood.* 109:3529–3537. http://dx.doi.org/10.1182/blood-2006-05-021402

Kuijpers, T.W., E. van de Vijver, M.A. Weterman, M. de Boer, A.T. Tool, T.K. van den Berg, M. Moser, M.E. Jakobs, K. Seeger, O. Sanal, et al. 2009. LAD-1/variant syndrome is caused by mutations in FERMT3. *Blood.* 113:4740–4746. http://dx.doi.org/10.1182/blood-2008-10-182154

Li, H., B. Handsaker, A. Wysoker, T. Fennell, J. Ruan, N. Homer, G. Marth, G. Abecasis, and R. Durbin; 1000 Genome Project Data Processing Subgroup. 2009. The Sequence Alignment/Map format and SAMtools. *Bioinformatics.* 25:2078–2079. http://dx.doi.org/10.1093/bioinformatics/btp352

Malinin, N.L., L. Zhang, J. Choi, A. Ciocea, O. Razorenova, Y.Q. Ma, E.A. Podrez, M. Tosi, D.P. Lennon, A.I. Caplan, et al. 2009. A point mutation in KINDLIN3 ablates activation of three integrin subfamilies in humans. *Nat. Med.* 15:313–318. http://dx.doi.org/10.1038/nm.1917

McDowall, A., L. Svensson, P. Stanley, I. Patzak, P. Chakravarty, K. Howarth, H. Sabnis, M. Briones, and N. Hogg. 2010. Two mutations in the KINDLIN3 gene of a new leukocyte adhesion deficiency III patient reveal distinct effects on leukocyte function in vitro. *Blood.* 115:4834–4842. http://dx.doi.org/10.1182/blood-2009-08-238709

Miller, S.A., D.D. Dykes, and H.F. Polesky. 1988. A simple salting out procedure for extracting DNA from human nucleated cells. *Nucleic Acids Res.* 16:1215. http://dx.doi.org/10.1093/nar/16.3.1215

Minato, N., K. Kometani, and M. Hattori. 2007. Regulation of immune responses and hematopoiesis by the Rap1 signal. *Adv. Immunol.* 93:229–264. http://dx.doi.org/10.1016/S0065-2776(06)93006-5

Naldini, L., U. Blömer, P. Gallay, D. Ory, R. Mulligan, F.H. Gage, I.M. Verma, and D. Trono. 1996. In vivo gene delivery and stable transduction of nondividing cells by a lentiviral vector. *Science.* 272:263–267. http://dx.doi.org/10.1126/science.272.5259.263

Nurden, A., and P. Nurden. 2011. Advances in our understanding of the molecular basis of disorders of platelet function. *J. Thromb. Haemost.* 9(Suppl 1): 76–91. http://dx.doi.org/10.1111/j.1538-7836.2011.04274.x

Pasvolsky, R., S.W. Feigelson, S.S. Kilic, A.J. Simon, G. Tal-Lapidot, V. Grabovsky, J.R. Crittenden, N. Amariglio, M. Safran, A.M. Graybiel, et al. 2007. A LAD-III syndrome is associated with defective expression of the Rap-1 activator CalDAG-GEFI in lymphocytes, neutrophils, and platelets. *J. Exp. Med.* 204:1571–1582.

Raaijmakers, J.H., and J.L. Bos. 2009. Specificity in Ras and Rap signaling. *J. Biol. Chem.* 284:10995–10999. http://dx.doi.org/10.1074/jbc.R800061200

Raslova, H., E. Komura, J.P. Le Couédic, F. Larbret, N. Debili, J. Feunteun, O. Danos, O. Albagli, W. Vainchenker, and R. Favier. 2004. FLI1 monoallelic expression combined with its hemizygous loss underlies Paris-Trousseau/Jacobsen thrombopenia. *J. Clin. Invest.* 114:77–84. http://dx.doi.org/10.1172/JCI21197

Reverter, J.C., S. Béguin, H. Kessels, R. Kumar, H.C. Hemker, and B.S. Coller. 1996. Inhibition of platelet-mediated, tissue factor-induced thrombin generation by the mouse/human chimeric 7E3 antibody. Potential implications for the effect of c7E3 Fab treatment on acute thrombosis and "clinical restenosis". *J. Clin. Invest.* 98:863–874. http://dx.doi.org/10.1172/JCI118859

Robert, P., M. Canault, C. Farnarier, A. Nurden, C. Grosdidier, V. Barlogis, P. Bongrand, A. Pierres, H. Chambost, and M.C. Alessi. 2011. A novel leukocyte adhesion deficiency III variant: kindlin-3 deficiency results in integrin- and nonintegrin-related defects in different steps of leukocyte adhesion. *J. Immunol.* 186:5273–5283. http://dx.doi.org/10.4049/jimmunol.1003141

Stadtmann, A., L. Brinkhaus, H. Mueller, J. Rossaint, M. Bolomini-Vittori, W. Bergmeier, H. Van Aken, D.D. Wagner, C. Laudanna, K. Ley, and A. Zarbock. 2011. Rap1a activation by CalDAG-GEFI and p38 MAPK is involved in E-selectin-dependent slow leukocyte rolling. *Eur. J. Immunol.* 41:2074–2085. http://dx.doi.org/10.1002/eji.201041196

Stefanini, L., R.C. Roden, and W. Bergmeier. 2009. CalDAG-GEFI is at the nexus of calcium-dependent platelet activation. *Blood.* 114:2506–2514. http://dx.doi.org/10.1182/blood-2009-04-218768

Stefanini, L., Y. Boulaftali, T.D. Ouellette, M. Holinstat, L. Désiré, B. Leblond, P. Andre, P.B. Conley, and W. Bergmeier. 2012. Rap1-Rac1 circuits potentiate platelet activation. *Arterioscler. Thromb. Vasc. Biol.* 32:434–441. http://dx.doi.org/10.1161/ATVBAHA.111.239194

Stolla, M., L. Stefanini, P. André, T.D. Ouellette, M.P. Reilly, S.E. McKenzie, and W. Bergmeier. 2011a. CalDAG-GEFI deficiency protects mice in a novel model of Fcγ RIIA-mediated thrombosis and thrombocytopenia. *Blood.* 118:1113–1120. http://dx.doi.org/10.1182/blood-2011-03-342352

Stolla, M., L. Stefanini, R.C. Roden, M. Chavez, J. Hirsch, T. Greene, T.D. Ouellette, S.F. Maloney, S.L. Diamond, M. Poncz, et al. 2011b. The kinetics of αIIbβ3 activation determines the size and stability of thrombi in mice: implications for antiplatelet therapy. *Blood.* 117:1005–1013. http://dx.doi.org/10.1182/blood-2010-07-297713

Stone, J.C. 2011. Regulation and Function of the RasGRP Family of Ras Activators in Blood Cells. *Genes Cancer.* 2:320–334. http://dx.doi.org/10.1177/1947601911408082

Svensson, L., K. Howarth, A. McDowall, I. Patzak, R. Evans, S. Ussar, M. Moser, A. Metin, M. Fried, I. Tomlinson, and N. Hogg. 2009. Leukocyte adhesion deficiency-III is caused by mutations in KINDLIN3 affecting integrin activation. *Nat. Med.* 15:306–312. http://dx.doi.org/10.1038/nm.1931

van de Vijver, E., A. Maddalena, O. Sanal, S.M. Holland, G. Uzel, M. Madkaikar, M. de Boer, K. van Leeuwen, M.Y. Köker, N. Parvaneh, et al. 2012. Hematologically important mutations: leukocyte adhesion deficiency (first update). *Blood Cells Mol. Dis.* 48:53–61. http://dx.doi.org/10.1016/j.bcmd.2011.10.004

van der Meijden, P.E., M.A. Feijge, F. Swieringa, K. Gilio, R. Nergiz-Unal, K. Hamulyák, and J.W. Heemskerk. 2012. Key role of integrin α(IIb)β(3) signaling to Syk kinase in tissue factor-induced thrombin generation. *Cell. Mol. Life Sci.* 69:3481–3492. http://dx.doi.org/10.1007/s00018-012-1033-2

Wang, K., M. Li, and H. Hakonarson. 2010. ANNOVAR: functional annotation of genetic variants from high-throughput sequencing data. *Nucleic Acids Res.* 38:e164. http://dx.doi.org/10.1093/nar/gkq603

Zhang, G., B. Xiang, S. Ye, M. Chrzanowska-Wodnicka, A.J. Morris, T.K. Gartner, S.W. Whiteheart, G.C. White II, S.S. Smyth, and Z. Li. 2011. Distinct roles for Rap1b protein in platelet secretion and integrin αIIbβ3 outside-in signaling. *J. Biol. Chem.* 286:39466–39477. http://dx.doi.org/10.1074/jbc.M111.239608